Strong electrocaloric effect in lead-free 0.65Ba(Zr0.2Ti0.8)O3-0.35(Ba0.7Ca0.3)TiO3 ceramics obtained by direct measurements

Mehmet Sanlialp, V.V. Shvartsman, Matias Acosta, Brahim Dkhil, D.C. Lupascu

Applied Physics Letters

Strong electrocaloric effect in lead-free $0.65Ba(Zr_{0.2}Ti_{0.8})O_3$-$0.35(Ba_{0.7}Ca_{0.3})TiO_3$ ceramics obtained by direct measurements

Cite as: Appl. Phys. Lett. **106**, 062901 (2015); https://doi.org/10.1063/1.4907774
Submitted: 11 December 2014 . Accepted: 28 January 2015 . Published Online: 09 February 2015

Mehmet Sanlialp, Vladimir V. Shvartsman, Matias Acosta, Brahim Dkhil, and Doru C. Lupascu

Strong electrocaloric effect in lead-free $0.65Ba(Zr_{0.2}Ti_{0.8})O_3$-$0.35(Ba_{0.7}Ca_{0.3})TiO_3$ ceramics obtained by direct measurements

Mehmet Sanlialp,[1] Vladimir V. Shvartsman,[1] Matias Acosta,[2] Brahim Dkhil,[3] and Doru C. Lupascu[1]

[1]*Institute for Materials Science and Center for Nanointegration Duisburg-Essen (CENIDE), University of Duisburg-Essen, Universitätsstraße 15, 45141 Essen, Germany*
[2]*Institute of Materials Science, Technische Universität Darmstadt, Alarich-Weiss Str. 2, 64287 Darmstadt, Germany*
[3]*Laboratoire Structures Propriétés et Modélisation des Solides, UMR CNRS 8580, Université Paris-Saclay, CentraleSupélec, 92295 Chatenay-Malabry Cedex, France*

(Received 11 December 2014; accepted 28 January 2015; published online 9 February 2015)

Solid solutions of $(1-x)Ba(Zr_{0.2}Ti_{0.8})O_3$-$x(Ba_{0.7}Ca_{0.3})TiO_3$ promise to exhibit a large electrocaloric effect (ECE), because their Curie temperature and a multiphase coexistence region lie near room temperature. We report on direct measurements of the electrocaloric effect in bulk ceramics $0.65Ba(Zr_{0.2}Ti_{0.8})O_3$-$0.35(Ba_{0.7}Ca_{0.3})TiO_3$ using a modified differential scanning calorimeter. The adiabatic temperature change reaches a value of $\Delta T_{EC} = 0.33$ K at ~65 °C under an electric field of 20 kV/cm. It remains sizeable in a broad temperature interval above this temperature. Direct measurements of the ECE proved that the temperature change exceeds the indirect estimates derived from Maxwell relations by about ~50%. The discrepancy is attributed to the relaxor character of this material. © *2015 AIP Publishing LLC*. [http://dx.doi.org/10.1063/1.4907774]

During the last several years, an increased interest has been paid to the electrocaloric effect (ECE) in ferroelectric materials as a route to develop small, effective, low cost, and environmentally friendly solid-state refrigerators.[1,2] The ECE is defined as an adiabatic and reversible temperature change of a dielectric material when an electric field is applied or removed.[3] If the exchange of heat with the environment is enabled, it defines the change of entropy as a function of the applied electric field under isothermal conditions.[4,5]

Since Mischenko *et al.* reported on the giant electrocaloric effect in $PbZr_{0.95}Ti_{0.05}O_3$ thin films in 2006,[6] the ECE has been reported for many different ferroelectric materials such as thick and thin films,[7–10] polymers,[11,12] bulk ceramics,[13,14] and single crystals.[15,16] In general, the ECE peaks are a few degrees above the ferroelectric-paraelectric phase transition.[1] The largest values have been achieved for thin films,[10] where much higher electric fields can be applied than to bulk materials. However, for application, the heating/cooling capacity is the key factor. Hence, bulk materials, which have large enough heating/cooling capacity, are better suitable for mid- and large-scale cooling applications.[1] To compare the ECE in different materials, the ratio between induced temperature change and applied field, $\Delta T_{EC}/\Delta E$, called the electrocaloric strength, has been introduced.[17] This parameter is independent of the geometrical shape and size of the samples.[1]

In many cases, the EC temperature change ΔT_{EC}^{ID} has not been measured directly, but rather estimated from the temperature dependences of polarization using Maxwell's relation[3] $\left(\frac{\partial P}{\partial T}\right)_{E,\sigma} = \left(\frac{\partial S}{\partial E}\right)_{T,\sigma}$

$$\Delta T_{EC}^{ID} = -T \int_{E_1}^{E_2} \frac{1}{C_{E,\sigma}} \left(\frac{dP}{dT}\right)_{E,\sigma} dE. \quad (1)$$

Here, P is the polarization, T is the temperature, E_1 and E_2 are starting and final values of the applied electric field, and $C_{E,\sigma}$ is the heat capacity. However, this estimate can be strictly applied to bulk monodomain single crystals only. In the case of multidomain ferroelectrics or non-ergodic systems, such as relaxors, only a qualitative agreement can be expected. Therefore, direct measurements of the EC effect must be performed.[1,3] As an example, Lu *et al.* compared direct and indirect ECE measurements on a polyvinylidene fluoride (PVDF)-based relaxor ferroelectric polymer and found that neither the magnitude nor even the temperature dependences match.[11]

Materials characterized by the coexistence of multiple states with different polarization orientations involving similar free energies are of particular interest. Field induced transformations of domain structures in these materials should be accompanied by large entropy changes and, correspondingly, by large ECE.[1] This arises in relaxors or ferroelectrics when two or more states with different symmetry have similar free energy. In the latter case, the best known example is the morphotropic phase boundary (MPB) between compounds with tetragonal and rhombohedral symmetry in the $PbZrO_3$-$PbTiO_3$ or $Pb(Mg_{1/3}Nb_{2/3})O_3$-$PbTiO_3$ (PMN-PT) solid solutions. Indeed, a relatively large electrocaloric (EC) temperature change has been reported for PMN-PT compositions near its MPB.[18–20] However, the large content of environmentally hazardous lead in these materials is a serious limitation for its industrial application according to regulation acts of the EU and other countries.[21] Therefore, environmentally friendly lead-free alternatives are desired.

Among the promising materials are solid solutions between $Ba(Zr,Ti)O_3$ and $(Ba,Ca)TiO_3$. In particular, the $(1-x)Ba(Zr_{0.2}Ti_{0.8})O_3$–$x(Ba_{0.7}Ca_{0.3})TiO_3$ (BZT-BCT) system has attracted a lot of attention due to its excellent electromechanical properties.[22–24] Its relatively low Curie

temperature lets one expect a large ECE response around room temperature, which is important for technological application. A particular feature of this system is the existence of a phase convergence region where four phases: paraelectric cubic, ferroelectric rhombohedral, ferroelectric tetragonal, and ferroelectric orthorhombic phases, meet.[25]

There have been several reports on the ECE in BZT-BCT ceramics and single crystals, but most of them have dealt with the indirect estimate of the ECE.[26–29] The direct measurements reported by Wang *et al.* for BZT-BCT ceramics with $x = 0.07$ were performed in non-adiabatic and non-equilibrium conditions.[29] The maximal ECE temperature change, ΔT_{ECE}, of 0.55 K was recorded for an applied field of 40 kV/cm at $T = 85\,^{\circ}C$. The authors found a very large discrepancy between the indirectly estimated and the directly measured ΔT_{ECE}. This was attributed to non-adiabatic conditions of the experiment resulting in a heat exchange with the environment.[29] Thus, direct ECE measurements in the BZT-BCT system have to be performed and correlated with indirect estimates based on Maxwell's relations.

In this letter, we report on direct measurements of the EC effect in lead-free $0.65Ba(Zr_{0.2}Ti_{0.8})O_3$-$0.35(Ba_{0.7}Ca_{0.3})TiO_3$ (BZT-35BCT) ceramics.

The $0.65Ba(Zr_{0.2}Ti_{0.8})O_3$-$0.35(Ba_{0.7}Ca_{0.3})TiO_3$ ceramic samples were synthesized by the conventional solid state reaction route. The details of sample preparation are reported elsewhere.[24] Before performing the measurements, the samples were ground to a thickness of 0.39 mm and sputtered with 100 nm Pt/Pd electrodes on both faces. The temperature dependence of the dielectric permittivity was measured in the range of 300–420 K at frequencies from 1 Hz to 1 MHz using a Solartron 1260 impedance analyzer with a dielectric interface 1296. Temperature dependent polarization versus electric field, $P(E)$, hysteresis loops were recorded at 100 Hz frequency using a custom built Sawyer-Tower circuit. The $P(E)$ measurements were performed in the temperature range of 25 °C–100 °C with an interval of 5 °C.

The direct EC measurements were carried out with a modified Differential Scanning Calorimeter (Netzsch, DSC 204). A similar method has been used by other groups.[4,31] A special sample cell with two spring loaders and thin varnished constantan wires was developed in order to apply the voltage to the sample. Figure 1(a) shows the modified DSC cell. Alumina crucibles, painted with silver in the inner side, were used in order to prevent electrical contact with the DSC sensor. While the spring loaders provided better contact between a sample and DSC sensors, they resulted in thermal losses during measurement. To evaluate the thermal loss factor, we performed reference measurements on four in-parallel connected small resistors. Figure 1(b) shows the temperature dependence of the thermal loss factor, K. From room temperature up to 100 °C, it is nearly linearly dependent on temperature and saturates above 100 °C. The ECE measurements were performed from 20 °C to 100 °C. Each temperature point was reached at 10 °C/min rate. Thereafter, the sample was kept for 30 min to stabilize the temperature before the ECE measurement started. The *dc* electric field with magnitude 10, 15, and 20 kV/cm was applied for 100 s and removed for 100 s at each measurement points. Heat

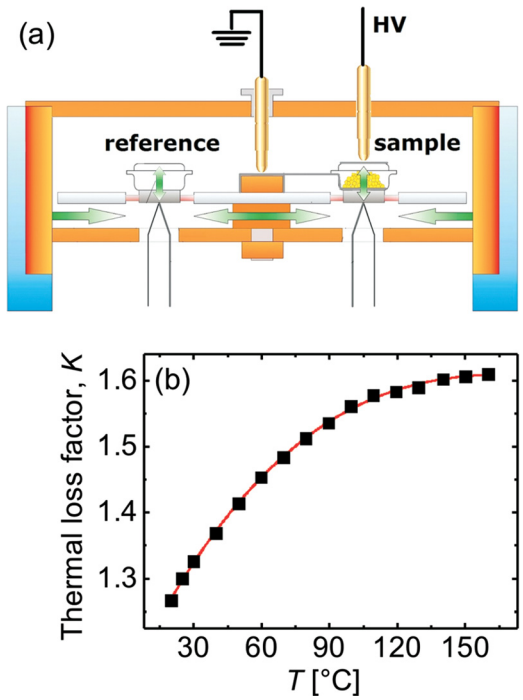

FIG. 1. (a) Modified DSC cell with two spring loaders. The sample is in the inner side of an alumina crucible (right) and a short wire is connected to the center where the second spring loader is connected to the circuit. (b) Thermal loss correction factor must be considered to compensate the heat losses during ECE measurements. The line shows a 3rd order polynomial fit to the experimental points.

capacity measurements were carried out with the same DSC setup, but using a standard cell.

Figure 2 introduces the temperature dependent relative permittivity measured at different frequencies upon heating. The $\varepsilon(T)$ curves show a broad maximum. Its position systematically shifts from 68 to 66 °C as the frequency decreases from 1 MHz to 1 Hz. Such behavior can be attributed to the weak relaxor properties of the parent $Ba(Zr_{0.2}Ti_{0.8})O_3$ composition.[30]

The $P(E)$ hysteresis loops measured at different temperatures are shown in Figure 3(a). One can see that both the remanent polarization (Fig. 3(b)) and coercive field decrease when approaching the Curie temperature, T_C (~65 °C). Moreover, the hysteresis does not disappear above T_C, slim hysteresis loops are observed even at 120 °C. Such behavior is a further indication of the relaxor character of the system

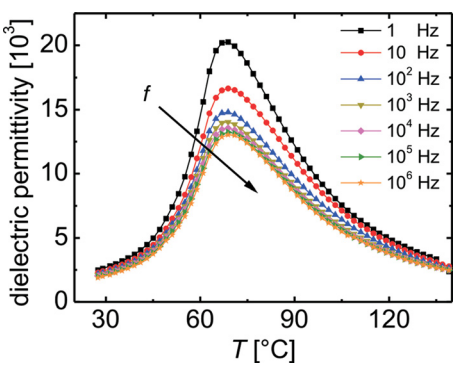

FIG. 2. Temperature dependences of the dielectric permittivity of BZT-35BCT ceramics measured at different frequencies upon heating.

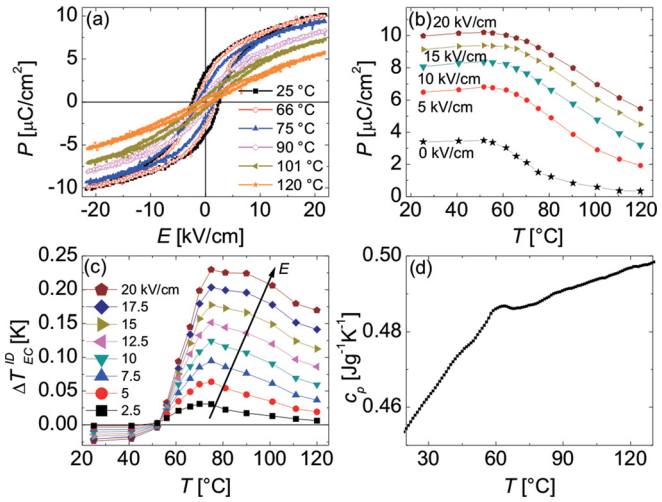

FIG. 3. (a) Electric field dependences of polarization measured at different temperatures. (b) Temperature dependences of polarization measured at different electric fields. (c) Temperature dependences of the EC effect estimated indirectly from P(T) dependences at different electric fields according Eq. (1). (d) Temperature dependences of specific heat capacitance measured on heating.

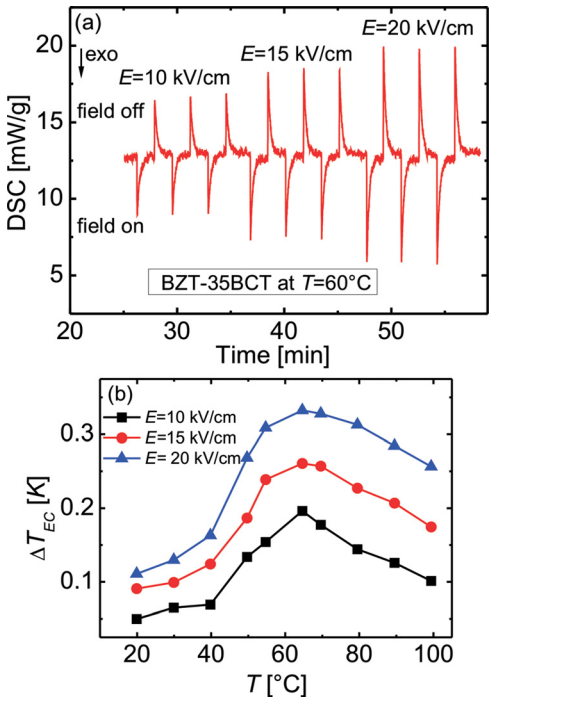

FIG. 4. (a) An example of electrocaloric measurements using the modified DSC. (b) Temperature dependences of the electrocaloric temperature change from the DCS measurements.

studied.[31] Temperature dependences of polarization at different electric fields were extracted (Fig. 3(b)) from the measured hysteresis loops. The remanent polarization shows a decay in the vicinity of T_C followed by a long tail in the nominally paraelectric phase. Non-zero polarization and residual piezoelectricity[24] above the Curie temperature, as reported earlier, can also be considered as the fingerprints for relaxor behavior of the system. For increased field, the anomaly on $P(T)$ at T_C is smeared out. Figure 3(c) shows the temperature dependences of the ECE, ΔT^{ID} is indirectly evaluated according to Eq. (1). At low field (2.5 kV/cm), the ECE reaches a maximum ($\Delta T^{ID} \sim 0.03$ K) at 70 °C, which is a few degrees above the transition temperature estimated from the dielectric measurements. As the applied field increases, ΔT^{ID} increases too and reaches ~0.23 K at 20 kV/cm. Concurrently, the maximum of the ECE shifts to higher temperature and becomes broader. A noticeable effect, $\Delta T^{ID} \sim 0.17$ K, was estimated at a temperature as high as 120 °C. The non-zero ΔT^{ID} far above T_C may be attributed either to an electric-field induced phase transition into a ferroelectric state and/or to the relaxor character of the material (see below).

Figure 3(d) presents the temperature dependence of the heat capacity, c_p. It is not constant over the studied temperature range as assumed in many other works and shows an anomaly near 60 °C, which corresponds to the phase transition between ferroelectric and paraelectric phases.[23]

Figure 4(a) displays a typical example of the direct ECE measurements with our setup (see Fig. 1). Application of an electric field results in an exothermic peak corresponding to heat release to the environment. By switching off the electric field, the DSC signal shows an endothermic peak corresponding to the heat absorption from the environment. Both exothermic and endothermic peaks are of similar magnitude, which verifies the reversibility of the effect. A contribution related to Joule heating can be neglected since the DSC signal returns to the baseline after switching the field on or off. Moreover, only a very small leakage current through the sample ($<10^{-8}$ A) was measured at each applied field. The magnitude of the peaks increases with increasing electric field.

To evaluate the specific heat exchange values, ΔQ, the area under exothermic and endothermic peaks was integrated. Then, the isothermal EC temperature change, ΔT_{EC}, was estimated for a given temperature according to the following equation:

$$\Delta T_{EC} = \frac{\Delta Q \cdot m_{ECE}}{c_p \cdot m_c} \cdot K, \tag{2}$$

where c_p is the specific heat capacity, m_{ECE} and m_c are masses of the sample at ECE and heat capacity measurements, and K is the thermal loss factor (Fig. 1(b)).

Figure 4(b) presents the ΔT_{EC} as a function of temperature at applied electric fields of 10, 15, and 20 kV/cm, featuring a broad peak at approximately 65 °C. The maximal temperature change of $\Delta T_{EC} = 0.33$ K was achieved for an electric field of 20 kV/cm. It is worth to compare the directly measured ECE with the indirect estimate from the $P(T)$ dependences. Qualitatively, both measurements show similar evolution of ECE upon heating: sharp increase of ΔT when approaching the phase transition, a maximum a few degrees above T_C, and a smooth decay at higher temperatures. Even at 100 °C (35 °C above the transition temperature), ΔT_{EC} is still about 75% of its maximal value. We believe that the broad electrocaloric peak extent into the paraelectric region is due to the relaxor character of BZT-35BCT.[32,33] This is in contrast, e.g., with data for pure $BaTiO_3$, where the strong ECE was observed only in the very vicinity (<10 K) of the Curie temperature.[17,34] Relaxors are well known to have a complex polar structure consisting of polar nanometer

TABLE I. Electrocaloric temperature change, electrocaloric strength, and corresponding measurement methods compared for different BZT-BCT compositions.

Material	T (°C)	ΔT_{max} (K)	ΔE (kV/cm)	$\Delta T_{max}/\Delta E$ (10^{-6}K × m/V)	Measurement method
BZT-35BCT ceramic (this work)	65	0.33	20	0.165	Direct DSC
BZT-35BCT ceramic (this work)	72	0.23	20	0.115	Indirect
BZT-35BCT ceramic[27]	80	0.27	20	0.135	Indirect
BZT-70BCT ceramic[27]	105	0.34	20	0.170	Indirect
BZT-55BCT single crystal[26]	131	0.46	12	0.383	Indirect
BZT-7BCT ceramic[29]	85	0.55	40	0.138	Direct non-adiabatic
BZT ceramics[37]	35	4.5	145	0.310	Direct adiabatic

regions (PNRs).[31] These PNRs do not disappear at T_m, but are preserved up to much higher temperatures.[31] This was verified for the studied material by observation of the slim $P(E)$ hysteresis loops at $T \gg T_m$. At zero field, PNRs are dynamically disordered, but an applied electric field can order them resulting in an entropy change and non-zero electrocaloric effect. Quantitatively, however, the ECE temperature change measured directly is approximately 50% larger than the value estimated according Eq. (1). This discrepancy can be rationalized by the existence of an extra contribution that is not taken into account by the Maxwell's relations. Above T_m, this contribution can be related to dynamic PNRs providing an additional entropy change upon electric field alignment. Correspondingly, the electrocaloric effect should be enhanced as compared to the ordinary ferroelectric-paraelectric phase transition.[11]

The situation is different for the ferroelectric state below T_m. Micron-sized domains were observed for BZT-BCT compositions with $x = 0.3$ and 0.4 at room temperature.[35,36] Under large enough electric field, these domains show a reversible transformation to a single domain state through an intermediate nanodomain state.[35] It is not excluded that such particular evolution also contributes to entropy changes and is responsible for the larger ECE value as indirectly estimated. An extra entropy contribution can be also expected in the multiphase region (just below T_m)[24,25] due to a field induced transformation between ferroelectric phases with different symmetries. However, we do not have enough experimental data to verify this assumption.

We observed that the directly measured effect reaches maximum values at lower temperature as compared to the indirect estimates. We suggest that the underlying reason for this discrepancy results from experimental errors in the temperature determination considering that both ECE and $P(E)$ measurements were performed with different setups.

Finally, we would like to compare our results with available literature data for the BZT-BCT system (Table I). Bai *et al.* indirectly evaluated the ECE for the nominally same composition and found a similar value, $\Delta T^{ID} \sim 0.27$ K, for slightly higher temperature.[27] According to these authors, the ECE increases with BCT content and reaches 0.34 K for BZT-70BCT, but at 105 °C.[27] Even larger values were reported for ceramics with small content of BCT, but at much higher electric fields.[29,37] The electrocaloric strength for various BZT-BCT compositions lies in the range of 0.15–0.20 K × mm/kV. Two results stand apart: indirect estimation for a single crystal BZT-55BCT by Singh *et al.*[26] and direct measurements of a micrometers thick slab of BZT ceramics by Qian *et al.*[37] showing two times larger electrocaloric strength. This can be due to the single crystalline nature of the sample in the former case and the particular experimental configuration in the latter one.

In summary, we have directly measured the electrocaloric effect in $0.65Ba(Zr_{0.2}Ti_{0.8})O_3$-$0.35(Ba_{0.7}Ca_{0.3})TiO_3$ ceramic using a modified differential scanning calorimeter. The maximal $\Delta T_{EC} = 0.33$ K was induced by an electric field of 20 kV/cm a few degrees above the Curie temperature. We found that using Maxwell's relation yields a 50% underestimation of the ECE in comparison to direct measurements. This can be related to nanodomain formation in the ferroelectric phase, existence of phase converge region close to T_m, and the relaxor character of the studied material. The latter also results in a broad ECE maximum. Relatively large ΔT_{EC} occurred in a broad temperature interval close to room temperature making this lead-free material attractive for environmental friendly solid-state cooling applications.

This work was supported by Deutsche Forschungsgemeinschaft, DFG, in the framework of the priority program "Ferroic Cooling" (SPP1599, Lu729/15-1) as well by the Leibniz program under RO954/22-1.

[1]M. Valant, Prog. Mater. Sci. **57**, 980 (2012).
[2]*Electrocaloric Materials: New Generation of Coolers*, edited by T. Correia and Q. Zhang (Springer, Berlin, Heidelber, 2014).
[3]R. Blinc, *Advanced Ferroelectricity* (Oxford University Press, 2011), pp. 203–214.
[4]G. Sebald, L. Seveyrat, D. Guyomar, L. Lebrun, B. Guiffard, and S. Pruvost, J. Appl. Phys. **100**, 124112 (2006).
[5]S. G. Lu and Q. Zhang, J. Adv. Dielectr. **2**, 1230011 (2012).
[6]A. S. Mischenko, Q. Zhang, J. F. Scott, R. W. Whatmore, and N. D. Mathur, Science **311**, 1270 (2006).
[7]B. Rožič, H. Uršič, J. Holc, M. Kosec, and Z. Kutnjak, Integr. Ferroelectr. **140**, 161 (2012).
[8]Y. Liu, I. C. Infante, X. Lou, D. C. Lupascu, and B. Dkhil, Appl. Phys. Lett. **104**, 012907 (2014).
[9]T. M. Correia, S. Kar-Narayan, J. S. Young, J. F. Scott, N. D. Mathur, R. W. Whatmore, and Q. Zhang, J. Phys. D: Appl. Phys. **44**, 165407 (2011).
[10]S. G. Lu, B. Rožič, Q. M. Zhang, Z. Kutnjak, X. Li, E. Furman, Lee J. Gorny, M. Lin, B. Malič, M. Kosec, R. Blinc, and R. Pirc, Appl. Phys. Lett. **97**, 162904 (2010).
[11]S. G. Lu, B. Rožič, Q. M. Zhang, Z. Kutnjak, R. Pirc, M. Lin, X. Li, and L. Gorny, Appl. Phys. Lett. **97**, 202901 (2010).
[12]P. F. Liu, J. L. Wang, X. J. Meng, J. Yang, B. Dkhil, and J. H. Chu, New J. Phys. **12**, 023035 (2010).
[13]X. Q. Liu, T. T. Chen, Y. J. Wu, and X. M. Chen, J. Am. Ceram. Soc. **96**, 1021 (2013).
[14]Z. Luo, D. Zhang, Y. Liu, D. Zhou, Y. Yao, C. Liu, B. Dkhil, X. Ren, and X. Lou, Appl. Phys. Lett. **105**, 102904 (2014).

[15]L. Luo, H. Chen, Y. Zhu, W. Li, H. Luo, and Y. Zhang, J. Alloys Compd. **509**, 8149 (2011).
[16]M. Valant, L. J. Dunne, A.-K. Axelsson, N. McN. Alford, G. Manos, J. Peräntie, J. Hagberg, H. Jantunen, and A. Dabkowski, Phys. Rev. B **81**, 214110 (2010).
[17]X. Moya, E. Stern-Taulats, S. Grossley, D. Gonzales-Alonso, S. Kar-Narayan, A. Planes, L. Manosa, and N. D. Mathur, Adv. Mater. **25**, 1360 (2013).
[18]Z. Feng, D. Shi, and S. Dou, Solid State Commun. **151**, 123 (2011).
[19]R. Chukka, J. W. Cheah, Z. Chen, P. Yang, S. Shannigrahi, J. Wang, and L. Chen, Appl. Phys. Lett. **98**, 242902 (2011).
[20]Y. He, X. M. Li, X. D. Gao, X. Leng, and W. Wang, Funct. Mater. Lett. **4**, 45 (2011).
[21]EU-Directive 2011/65/EU, "Restriction of the use of certain hazardous substances in electrical and electronic equipment (RoHS)," Off. J. Eur. Union **L 174**, 88 (2011).
[22]W. Liu and X. Ren, Phys. Rev. Lett. **103**, 257602 (2009).
[23]D. R. J. Brandt, M. Acosta, J. Koruza, and K. G. Weber, J. Appl. Phys. **115**, 204107 (2014).
[24]M. Acosta, N. Novak, W. Jo, and J. Rödel, Acta Mater. **80**, 48 (2014).
[25]D. S. Keeble, F. Benabdallah, P. A. Thomas, M. Maglione, and J. Kreisel, Appl. Phys. Lett. **102**, 092903 (2013).
[26]G. Singh, I. Bhaumik, S. Ganesamoorthy, R. Bhatt, A. K. Karnai, V. S. Tiwari, and P. K. Gupta, Appl. Phys. Lett. **102**, 082902 (2013).
[27]Y. Bai, X. Han, and L. Qiao, Appl. Phys. Lett. **102**, 252904 (2013).
[28]G. Singh, V. S. Tiwari, and P. K. Gupta, Appl. Phys. Lett. **103**, 202903 (2013).
[29]J. Wang, T. Yang, S. Chen, G. Li, Q. Zhang, and X. Yao, J. Alloys Compd. **550**, 561 (2013).
[30]V. V. Shvartsman, J. Zhai, and W. Kleemann, Ferroelectrics **379**, 301 (2009).
[31]A. A. Bokov and Z.-G. Ye, J. Mater. Sci. **41**, 31 (2006).
[32]Y. P. Shi and A. K. Soh, Acta Mater. **59**, 5574 (2011).
[33]J. Peräntie, H. N. Tailor, J. Hagberg, H. Jantunen, and Z.-G. Ye, J. Appl. Phys. **114**, 174105 (2013).
[34]N. Novak, Z. Kutnjak, and R. Pirc, EPL **103**, 47001 (2013).
[35]M. Zakhozheva, L. A. Schmitt, M. Acosta, J. Rödel, and H.-J. Kleebe, Appl. Phys. Lett. **105**, 112904 (2014).
[36]J. Gao, D. Xue, Y. Wang, D. Wang, L Zhang, X. Wu, S. Guo, H. Bao, C. Zhou, W. Liu, S. Hou, G. Xiao, and X. Ren, Appl. Phys. Lett. **99**, 092901 (2011).
[37]X.-S. Qian, H.-J. Ye, Y.-T. Zhang, H. Gu, X. Li, C. A. Randall, and Q. M. Zhang, Adv. Funct. Mater. **24**, 1300 (2014).